Manuscript Details

Manuscript number	AESCTE_2017_288
Title	Fault detection in operating helicopter drivetrain components based on support vector data description
Article type	Full length article

Abstract

The objective of the paper is to develop a vibration-based automated procedure dealing with early detection of mechanical degradation of helicopter drive train components using Health and Usage \mbox{Monitoring} Systems (HUMS) data. An anomaly-detection method devoted to the quantification of the degree of deviation of the mechanical state of a component from its nominal condition is developed. This method is based on an Anomaly Score (AS) formed by a combination of a set of statistical features correlated with specific damages, also known as Condition Indicators (CI), thus the operational variability is implicitly included in the model through the CI correlation. The problem of fault detection is then recast as a one-class classification problem in the space spanned by a set of CI, with the aim of a global differentiation between normal and anomalous observations, respectively related to healthy and supposedly faulty components. In this paper, a procedure based on an efficient one-class classification method that does not require any assumption on the data distribution, is used. The core of such an approach is the Support Vector Data Description (SVDD), that allows an efficient data description without the need of a significant amount of statistical data. Several analyses have been carried out in order to validate the proposed procedure, using flight vibration data collected from a H135, formerly known as EC135, servicing helicopter, for which micro-pitting damage on a gear was detected by HUMS and assessed through visual inspection. The capability of the proposed approach of providing better trade-off between false alarm rates and missed detection rates with respect to individual CI and to the AS obtained assuming jointly-Gaussian-distributed CI has been also analysed.

Keywords	HUMS; rotating machinery; fault detection; anomaly detection; gearbox diagnosis
Taxonomy	Vibration Analysis, System Fault Detection, Mechanical Vibration

Corresponding Author	Valerio Camerini
Corresponding Author's Institution	Airbus
Order of Authors	Valerio Camerini, Giuliano Coppotelli, Stefan Bendisch

Suggested reviewers	Jerome Antoni, Victor Girondin, Paula J. Dempsey

Submission Files Included in this PDF

File Name [File Type]

Review_letter_AESCTE_AAD_17.doc [Response to Reviewers]

AESCTE_Highlights.doc [Highlights]

2017_06_AESCT_AAD_Reviewed.pdf [Manuscript File]

To view all the submission files, including those not included in the PDF, click on the manuscript title on your EVISE Homepage, then click 'Download zip file'.

Ref: AESCTE_2017_288
Title: Fault detection in operating helicopter drivetrain components based on support vector data description
Journal: Aerospace Science and Technology
Authors: Valerio Camerini, PhD Student;
Giuliano Coppotelli, Assistant Professor;
Stefan Bendisch, R&D Engineer

Editor letter:
Dear Mr. Camerini,

Thank you for submitting your manuscript to Aerospace Science and Technology. We have completed the review of your manuscript. A summary is appended below. While revising the paper please consider the reviewers' comments carefully. We look forward to receiving your detailed response and your revised manuscript.

I look forward to receiving your revised manuscript as soon as possible.

Kind regards,

Professor Barakos
Associate Editor
Aerospace Science and Technology

Authors' Response:
We would like to thank the editor and the reviewers for their detailed work and useful comments. We improved the paper as to address most of the concerns of the reviewers. The responses to the reviewer’s comments are provided here along with the new amended paper.

Authors' Responses to Reviewers' comments

Reviewer 1 Comment # 1
In equation (1), it is not clear if the convolution applies to variable t only or to t and theta. In the latter case it is unconventional and the integral equation should be given explicitly instead of only its symbolic notation.

Authors' Reply:
Thanks for pointing this out, **we specified that the convolution applies only to the variable *t*** in the text and clarified the notation.

Reviewer 1 Comment # 2
In equation (2), the dependence of Ms1 and Ms2 on phi is missing.

Authors' Reply:
Fixed according to the observation.

Reviewer 1 Comment # 3
In section 2.1.3 (line 6), a reference is missing.

Authors' Reply:
Fixed according to the observation.

Reviewer 1 Comment # 4
As a general remark, the RMS and kurtosis indicators are simplisitic indicators. Why are other indicators not been tested, such as energy in frequency bands, amplitude of harmonics, modulation depth, etc? In addition, one drawback of the RMS value is to be extremely sensitive to operational condition (often more than to an incipient fault). These choices must be discussed.

Authors' Reply:
Justification for the choices has been made clearer in the article by expanding section 2.1.3 according to the suggested revision.

****

Reviewer 2 Comments # 1,2,6,10,11
- **Who is the corresponding author?**
- **Abstract should not contain parenthesis, except for acronyms.**
- **Figure 3 : please rescale between -40 and 40 if possible**
- **Adding a nomenclature at the beginning would be helpful**
- **Section 3.2 has only one subsection 3.2.1, it would help to add more subsections**
- **The role played by sigma (equation 27) is not detailed**

Authors' Reply:
Fixed according to the observations.

Reviewer 2 Comment # 3
The reason why SVM is preferred over other methods is not detailed enough. For example the author could highlight that the learning period is reduced compared with other methods or that the fitness error is reduced. Also the author could be more 'critical' when reviewing other methods. Without this, the reader reaches section 2.2, and does not understand why SVM is chosen.

Authors' Reply:

Thanks for this observation. **We highlighted crucial points and added further details in the comparison with other methods in the OCC framework** (Introduction section). We think this improved the clarity of our choices in the manuscript.

Reviewer 2 Comment # 4

The use of the word 'correlation' is not always appropriate. Correlation means linear dependance, which is a strong and testable assumption. I'm not sure that the author means 'linear dependance' whenever he writes correlation. Consider rephrasing.

Authors' Reply:
We realize that due to Pearson´s coefficient, the word correlation is in the statistical literature commonly associated with linear correlation. Probably it would be more proper for us to use the phrasing "statistical association between variables". However, the notion of "nonlinear correlation" appears also often in scientific literature. Besides, albeit the popular Spearman's rank correlation coefficient does not measure a linear relationship, it uses the word correlation. In the introduction, **we added a specific declaration of the use we make of the word and made explicit the distinction with "linear correlation"**, in the hope of improving clarity.

Reviewer 2 Comment # 5

All the section 2.1 brings little to help understanding the key contribution of this article. I would suggest to reduce it a lot:

Authors' Reply:
We revised the section in order to improve readability. All the notation and concepts are declared in order to explain the choices we made in the processing of the signal devoted to the extraction of a gear-related signature. For example, the concept of cycloergodicity is introduced to justify the estimation we made of the quantity s_g through the synchronous averaging process. Further, advanced concepts are used to justify processing choices with relation to constraints from, e.g., measurement equipment and to make the paper self-contained. **The link between the gear signature s_g and the estimation has been made explicit in equation 9 for the sake of clarity.**

Reviewer 2 Comment # 7

Figure 8 (a) : brackets in the legend should have a bold font? Also what is the number in the brackets?

Authors' Reply:
It was the variance of AUC and was used in the results analysis phase from the authors before further elaborating on AUC statistics. Thanks for pointing out that it was erroneously left in the legends without commenting it, **we provided to update the figures by removing that number,** since AUC statistics are later discussed in the paper.

Reviewer 2 Comment # 9

It is more or less assumed that the underlying distribution has a shape that can be described by a sum of gaussians, meaning that it cannot be for example a 'heavy tail' distribution. In the abstract, you said that you don't need to make assumptions on the shape of the distribution.

Authors' Reply:
We hope that the comments added in the introduction concerning the choice of SVDD as OCC have contributed to make this point clearer. We are not in fact estimating

the density of the target set, but employing a boundary description method which uses a Gaussian kernel to project the features in a higher dimensional space.

****

Highlights

- Methodology for automated mechanical fault detection in helicopter fleets.
- Feature extraction and fusion through machine learning methods are discussed.
- Validation on experimental data from real operating H135 helicopter is presented.

FAULT DETECTION IN OPERATING HELICOPTER DRIVETRAIN COMPONENTS BASED ON SUPPORT VECTOR DATA DESCRIPTION

V. Camerini *[a,b], G. Coppotelli[a], and S. Bendisch[b]

[a]*Department of Mechanical and Aerospace Engineering, University of Rome "La Sapienza", 00184 Rome, Italy*

[b]*Airbus Helicopters Germany, 86609 Donauwörth, Germany*

Abstract

The objective of the paper is to develop a vibration-based automated procedure dealing with early detection of mechanical degradation of helicopter drive train components using Health and Usage Monitoring Systems (HUMS) data. An anomaly-detection method devoted to the quantification of the degree of deviation of the mechanical state of a component from its nominal condition is developed. This method is based on an Anomaly Score (AS) formed by a combination of a set of statistical features correlated with specific damages, also known as Condition Indicators (CI), thus the operational variability is implicitly included in the model through the CI correlation. The problem of fault detection is then recast as a one-class classification problem in the space spanned by a set of CI, with the aim of a global differentiation between normal and anomalous observations, respectively related to healthy and supposedly faulty components. In this paper, a procedure based on an efficient one-class classification method that does not require any assumption on the data distribution, is used. The core of such an approach is the Support Vector Data Description (SVDD), that allows an efficient data description without the need of a significant amount of statistical data. Several analyses have been carried out in order to validate the proposed procedure, using flight vibration data collected from a H135, formerly known as EC135, servicing helicopter, for which micro-pitting damage on a gear was detected by HUMS and assessed through visual inspection. The capability of the proposed approach of providing better trade-off between false alarm rates and missed detection rates with respect to individual CI and to the AS obtained assuming jointly-Gaussian-distributed CI has been also analysed.

Nomenclature

AS	Anomaly Score
AUC	Area Under the Curve
CI	Condition Indicator
GMM	Gaussian Mixture Model
HUMS	Health and Usage Monitoring Systems
KRT	Kurtosis (fourth standardized statistical moment)
MD	Mahalanobis Distance
OM	Amplitude of harmonic component
RMS	Root Mean Square value
ROC	Receiver Operating Characteristic
SA	Synchronous Average
SVDD	Support Vector Data Description

*Corresponding author: valerio.camerini@uniroma1.it

1. Introduction

The problem of early fault detection is crucial in helicopter maintenance strategy. Early stage, undetected damage affecting critical sub-systems can progressively increase causing the system to fail. In the best case, such a scenario could result in increased operating costs for the machine owing to the required grounding time, maintenance and part replacement, as well as it could lead to dangerous accidents in some cases. The drive train sub-system is responsible for transferring power from the engines to the rotors, and represents a critical sub-system for the machine due to non-redundant load paths and the high variability of the dynamic loads acting on the components ([1]).

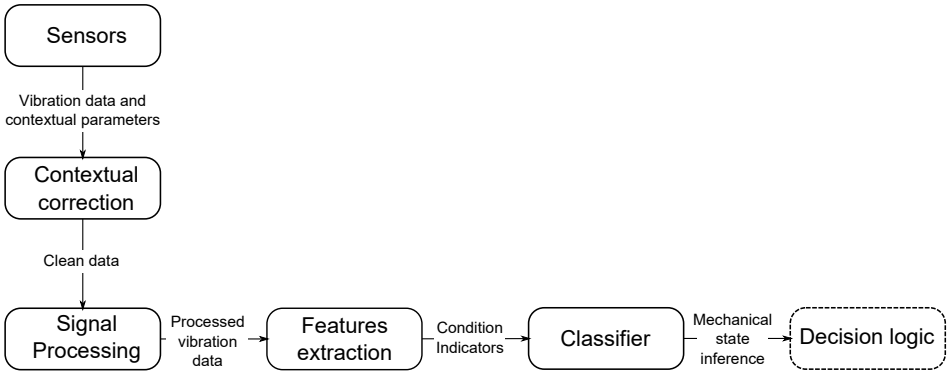

Figure 1: High level overview of HUMS diagnosis process.

As to ensure aircraft airworthiness, the system needs to be maintained following a prescribed preventive maintenance program, resulting in a burden to operating costs and aircraft availability. Therefore, Health and Usage Monitoring Systems (HUMS), defined as equipment/techniques/procedures by which selected incipient failure or degradation can be determined in [2], were introduced in the last decades in helicopter industry as a mean of increasing safety and reducing maintenance costs by enabling Condition Based Maintenance (CBM) ([3, 4]). Because damages are not directly observable, it is necessary to measure quantities which are affected by fault development. Mechanical degradation affects the vibration signature emitted from drive train rotating components. Moreover, technologies for measuring vibration signals are readily available. Therefore, it is common in the helicopter industry to equip rotating parts in the drive train with sensitive sensors (typically accelerometers) able of recording dynamic oscillation. The HUMS includes a transmission monitoring function which uses three types of data ([5]): accelerometer and tachometer signals, as well as contextual parameters such as airspeed, temperature and engine torque. Accelerometers are typically mounted on gearboxes and shaft bearings, tachometers on rotor shafts. The contextual parameters, when available, usually come from sensors which are part of other avionic/navigation systems than HUMS. Within the HUMS, a diagnosis logic is implemented in order to process a set of sensor signals by which the mechanical state of underlying assets is inferred. Figure 1 represents an overview of the diagnosis process. Sensor data are in a first step corrected for the contextual parameters. Invalid data, like noisy acquisitions or data recorded in unfavourable conditions (e.g. during run-ups or other non-stationary conditions of the machine) are rejected at this stage (contextual correction in figure 1). Features extraction consists of converting the raw sensor input in a metrics which is more informative about the state of the system ([6]), such features are commonly referred to as Condition Indicators (CI). Finally, CI are interpreted as an input to a classifier, with the aim of producing the most likely decision about the state of the monitored components. The inference may be as simple as deciding if a fault is present (fault detection), up to providing prognostic information on the remaining useful life for a given component. Such information is then passed to the overlying decision logic, supporting the maintenance decision process. Traditional HUMS ([7]) are based on univariate monitoring of each CI. The values of each CI are compared to an individual threshold, computed from fleet historical data. An alert is generated whenever any of the CI exceeds its threshold. However, the high variability of aerodynamic loads, transmission loads and operating conditions affect the vibration signature, resulting in high scattering of the CI values ([8, 9]). Therefore, despite the efforts in developing damage-sensitive features using advanced signal processing techniques, state-of-the-art HUMS are prone to increased false alarms ([10]). A novel approach to the CI analysis was developed in a five-year research program involving GE aviation ([10]), where multiple CI from fleet data are combined in a single Anomaly Score (AS). Such an AS represents the degree of deviation of an acquisition from the nominal state, defined using a Gaussian Mixture Models (GMM) based on the entire fleet multivariate data as a reference. Results revealed that this feature-level data fusion was capable of enhancing fault detection performance of classical HUMS analysis methods, neither requiring restrictions on operating conditions nor explicit modelling of their effects on the CI values. Contemporary, the research at Airbus Helicopters (AH) resulted in a different strategy, adopted in [11], where CI are combined in a so-called Health Indicator (HI) using the definition of Mahalanobis Distance. The HI are defined based on a set of CI for each component, and the nominal state definition relies on few acquisitions

following a maintenance action. Differently from [10], this method aims to model a baseline for each individual component, independently from fleet data, thus preventing the between-helicopters variability due to different configurations and installation tolerances ([12]) to mask local trends in the CI. However, an intrinsic limitation of the methodology is in the obvious impossibility of detecting manufacturing defects. Besides, Gaussian assumption of the CI distribution is required. Actually, the fault detection problem can be considered as a one-class classification problem, with the task of separating the normal (healthy) data samples from the faulty ones. Support Vector Description (SVDD) is an unsupervised machine learning method specifically developed for solving the one-class classification problem by Tax and Duin ([13]). SVDD solves the problem of data description given a set of training samples, from which the boundaries of the target distribution are learnt. This approach has been successfully employed in image classification problems, one-class pattern recognition, damage detection, batch process monitoring, etc. (e.g. [14–17]). Examples of the application of SVDD in machine condition monitoring are found in [18–21]. Differently from data description methods aiming to describe the target density (e.g. Gaussian Mixture Models or Parzen density estimation), boundary methods (as SVDD, K-centers [22] or Nearest Neighbors [23, 24]) aim to capture the boundaries of the target in the feature space, proving particulary useful when only few examples are available and they are poorly representative of the complete target class probability density in the feature space. Further, boundary methods are advantageous compared to reconstruction methods (e.g. k-means clustering, learning vector quantization, self-organizing maps, Principal Components Analysis or auto-encoder networks [24, 25]) in that they introduce lower bias on the obtained model description, and generally requires less tuning efforts ([24]). Among boundary description methods, SVDD proves particularly robust to training sets which are not fully representative of the test data ([24]). Since in the current application it is typically desired to learn a baseline from few training examples, which might often be insufficient to capture the full data density, SVDD is deemed a suitable data description method. In this paper, fault detection using HUMS data is recast as an anomaly detection problem in the space spanned by multiple CI as in [10]. In order to account for between-helicopters variability in the same fleet, individual component models are proposed as in [11]. The operational variability is implicitly accounted for in the model through the correlation induced within CI. The general notion of correlation is here used to indicate a causal or non-causal statistical relationship between random variables. The notion of linear correlation is explicitely made distinct whenever necessary. Since CI were preliminarily observed to be non-linearly correlated, with non-normal marginal distributions, a SVDD model is used for data description. The SVDD output is used as an AS, quantifying the degree of abnormality of an observation from the nominal distribution. The remainder of this paper is organised as follows. First, a theoretical background is given in Section 2. Extraction of CI from vibration data is introduced, then the basic SVDD model is presented and the proposed methodology described. In Section 3, the proposed methodology is evaluated on vibration data from a servicing H135 (formerly known as EC135) with a developing micro-pitting damage. Such data are collected in real operating conditions, extracted CI present therefore the associated scattering. It is shown that the developed algorithm can be applied in an operational framework, producing an AS which increases the separation between normal and faulty data with respect to individual CI and to a multivariate model based on Gaussian assumption. Finally, conclusions are made in Section 4.

2. Theoretical background

2.1. Extraction of Condition Indicators from vibration data

The general problem of CI extraction from accelerometers response in complex machinery is briefly introduced using a linear model, then, considering the specific case of gear signature extraction, the procedure adopted for defining related CI is described. Among the many techniques proposed in literature for gear local fault detection (see, e.g. [26–30], statistical features extraction based on the so-called synchronous average signal is considered in this work for its simplicity and proved effectiveness. Methods based on enhancing the impulsivity of damaged teeth impacts like the one proposed by Combet and Gelman in [31], based on Spectral Kurtosis (SK) optimal filtering [32, 33] were not considered. On one side, the limited sampling frequency of available sensors poses a strong constraint on the signal bandwidth, preventing from detecting high-frequency resonant bands. On the other hand, the short-time duration of the acquisitions results in a relatively gross spectral resolution of the estimated time-frequency energy distribution of the signal.

2.1.1 Model of accelerometer response

The vibration response of the structural components to the operational excitation is assumed to be linear in the considered frequency range. The linear model for the response $x_j(t,\theta)$ at position j in a mechanical environment characterised by multiple vibration sources, with t and θ respectively the short time-scale associated with measurements and the long time-scale characteristic of the monitoring process across machine's life, is then given as ([34]):

$$\begin{aligned} x_j(t,\theta) = &\sum_{i=1}^{NF} h_{ij}^F(t,\theta) * F_i(t,\theta) + \\ &+ \sum_{i=1}^{NI} h_{ij}^I(t,\theta) * I_i(t,\theta) + \\ &+ h_j^S(t,\theta) * m(t,\theta) + n_j(t,\theta), \end{aligned} \tag{1}$$

where $*$ denotes the convolution operation in the measurement time variable t. In the following, the dependency of the vibration signal over θ, reflecting changes in the measured vibration due to long-term changes in the state of the machine, is dropped from the notation. The response is then given as the sum of NF fault-related signals $F_i(t)$ and NI interfering machinery signals $I_i(t)$ respectively convolved with the impulse response functions $h_{ij}^F(t)$ and $h_{ij}^I(t)$. The term $h_j^S(t) * m(t)$ explicitly introduces in the model the modal response at location j due to all remaining excitation sources from normal machine operation and imperfections. Finally, $n_j(t)$ models the ambient and sensor noise. From equation (1), the measured acceleration at the transducer location is the convolutive mixture of multiple sources. The identification of fault-related signatures requires isolating them from the rest of the signal, filtering out those interfering components related to the functioning of the healthy state machinery in its actual operating environment. Therefore, an understanding of the properties of fault or normal vibration is mandatory ([35]). Besides, the model of equation (1) includes the dependency of the measured vibration on the mode shapes of the system (and consequently the sensor position as well), the operating state of the machine and the transmission paths from the sources to the accelerometer.

2.1.2 Gear signature extraction

Referring to a pair of mating gears composed of wheels connected to rotating shafts, the dynamic excitation arising from gear motion can be decomposed in a deterministic part and a random stochastic one. The former is mainly due to meshing impacts and it is composed of a contribution with period equal to the meshing period of the mating gears, amplitude modulated from shaft-synchronous components, and a contribution having the common wheels period ([36]). The latter can be modeled as a white noise process arising from sliding contact between teeth undergoing periodic gear mesh force amplitude modulation plus white noise amplitude modulated at shaft frequency connected to imperfections as, e.g. wear [37]. Therefore, the dynamic excitation from the gear, $s_g(t)$, reads:

$$s_g(t) = d_g(t) + r_g(t), \tag{2}$$

where $d_g(t)$ and $r_g(t)$ are the deterministic and random contributions to $s_g(t)$. The excitation source is angle-synchronous with the machine cycles, rather than time-synchronous. Introducing the variable $\phi(t)$ representing the reference shaft rotation angle as a function of time and allowing for time-varying rotational frequency, it is possible to write $s_g(t) = s_g(\phi(t))$. Here $\phi(t) = \int_0^t 2\pi f_s(\tau)d\tau$ connects the angular and time domain through the instantaneous rotational frequency $f_s(t)$ of the shaft. The deterministic contribution $d_g(t)$ from equation (2) can be thus expressed as (dropping the dependency of the shaft rotation angle on time in order to simplify the notation):

$$\begin{aligned} d_g(t) = &Q_d(f_s(t))(1 + M_{s1}(\phi) + \\ &+ M_{s2}(\phi) + M_i(\phi)) \sum_k a_k cos(kZ\phi), \end{aligned} \tag{3}$$

where $Q_d(f_s(t))$ is a monotonically increasing modulation function with respect to the shaft speed as introduced in [37], accounting for long-term non-stationarities, Z is the number of teeth of the gear, a_k the kth Fourier coefficient of the angle-periodic gear mesh harmonic, $M_{s1}(\phi)$ and $M_{s2}(\phi)$ the amplitude modulation due to the wheels rotation and $M_i(\phi)$ the amplitude modulation due to an eventual local gear fault. The non-deterministic contribution to the gear signal can be modeled as:

$$\begin{aligned} r_g(t) = &Q_{r1}(f_s(t))W_1(t) \sum_k a_k cos(kZ\phi) + \\ &+ Q_{r2}(f_s(t))W_2(t) \sum_j a_j cos(j\phi), \end{aligned} \tag{4}$$

in which the white noise processes $W_1(t)$ and $W_2(t)$ are modulated by angle-periodic functions of period equal to that of the shaft and to that of the gear mesh, and the speed-dependent energy modulation caused by the change of machine power intake [37] is accounted for in terms $Q_{r1}(f_s(t))$ and $Q_{r2}(f_s(t))$. Specifically, the first term in (4) is directly related to the gear surface roughness [38], whereas the second one is the

stochastic contribution related to load, random stiffness fluctuations, machining errors, etc. Although accounting for a significantly smaller contribution to the signal energy when compared to the deterministic part, the random part of the gear signal can highlight information about early damaged teeth generating impulsive contacts. Such small-amplitude repetitive impulses can be detected using second order cyclostationary tools [36] and exploiting high-frequency resonant bands in which the signal to noise ratio is high enough for allowing signal identification and extraction. The measured response signal can be expressed as:

$$x_g(t) = h_g(t) * s_g(t), \tag{5}$$

where $h_g(t)$ denotes the linear time invariant (LTI) impulse response representing the transfer path (TP) from the source location of the dynamic excitation to the measurement point location. It is assumed that for the operating conditions considered in this work, the fluctuation of the reference shaft rotational frequency is sufficiently small during the observation time. This implies that:

- The modulation terms $Q_d(f_s(t))$, $Q_{r1}(f_s(t))$ and $Q_{r2}(f_s(t))$ can be considered constant during the observation time;
- The LTI filtering of the transfer path introduces negligible distortion in the angle-periodic signal, i.e. the amplitude and phase delay of the generic response component in the shaft order domain can be considered constant during the observation time.

Consequently, owing to the periodicity of the modulation functions, the response signal due to the gear excitation can be expressed as [36]:

$$x_g(\phi) = p_1(\phi) + p_2(\phi) + p_{1,2}(\phi) + r(\phi), \tag{6}$$

with p_i denoting periodic contributions synchronous with the i-th shaft rotation, $p_{1,2}$ the contribution from the common wheels period, and $r(\phi)$ the stochastic one, that is generally small compared to the deterministic one. Moreover, the random part is discarded from the analysis due to the very same operational limitations explained in the beginning of section 2.1.2, which make difficult to separate the random part of the gear signal from the background noise. In order to extract the gear contribution $x_g(\phi)$ from the whole response signal $x_j(t)$, it is then necessary to isolate the angle-periodic contribution. Such an operation requires in general two main steps, namely angle-synchronization and filtering. In angle synchronization the measured vibration signal $x_j(t)$, sampled synchronously with time, is resampled in the angle-domain. This step is achieved using computed order tracking (COT) techniques [39]. Such techniques are based on reconstructing through interpolation (second-order polynomial in [39]) the time-angle relationship based on associating specific time instants to specific fractions of shaft revolutions. This association can be made both using an external trigger signal (e.g. keyphasor pulses) or, under some conditions, extracting the speed progression directly from the vibration signal as in [40]. After the time-angle relationship is given, the time-sampled response signal, $x_j(t)$, can be resampled for constant angle increment values. The resulting signal $x_j(\phi)$ is then described as a function of a given shaft angle ϕ. In this work, order tracking is performed using keyphasor pulses provided from a magnetic pickup which is part of helicopter HUMS equipment, whereas cubic spline interpolation is used for resampling the vibration signal recorded from an accelerometer. The second step, consisting of the filtering operation can be efficiently performed through synchronous average in the angle domain. The synchronous average (SA) procedure requires prior knowledge of the period to be extracted, and it consists of averaging N_{SA} distinct periods of the considered signal. This synchronous average corresponds to an estimation of the first-order cyclostationary part (CS1) of the signal of cycle equal to the considered averaging period [36]. Under the assumption of cycloergodicity, the ensemble average can be confused in facts with cycle averaging [36]. Namely, the synchronous average of an angular-sampled signal $x(\phi)$ of angular cycle Φ is estimated as:

$$x_{SA}(\phi) = \frac{1}{N_{SA}} \sum_{k=0}^{N_{SA}} x(\phi + k\Phi). \tag{7}$$

It can be shown that the attenuation of the white noise in the signal is proportional to $1/\sqrt{N_{SA}}$. When described in angular-frequency domain, the synchronous average operation corresponds to a comb-filter applied to the signal, with unit gain for multiples of the basic cycle Φ and transfer function of modulus:

$$|H_{SA}(\gamma)| = \left|\frac{sin(\pi\gamma\Phi N_{SA})}{N_{SA} sin(\pi\gamma\Phi)}\right|, \tag{8}$$

where γ is the equivalent of a frequency for the angular-domain signal (i.e. γ represents orders of the reference shaft when $\Phi = 1$). Equation (8) shows that the number of averages determine not only the attenuation of non-synchronous components, but also the position of the zeros of the filter and its maxima, therefore it might be worth considering N_{SA} as a design parameter when strong deterministic, known

components need to be attenuated in the signal. Under the assumption of small speed fluctuations, the gear signal related to wheel i can then be estimated from the re-sampled response signal $x_j(\phi)$ as:

$$\hat{s}_g(\phi) \approx p_i(\phi) \approx \frac{1}{N_{SA}} \sum_{k=0}^{N_{SA}} x_j(\phi - k\Phi_i) = x_{SA}(\phi), \tag{9}$$

being Φ_i the cycle of wheel i and the sensor j the one which (among available sensors) minimizes the transfer path from the source of interest. The estimation $\hat{s}_g(\phi)$ of $s_g(\phi)$ is representative of the gear source signature, having neglected the mutual wheel modulation effects term $p_{1,2}(\phi)$, due to the common period of the mating gears being (usually, but not necessarily) too long for obtaining a proper number of cycles to be averaged from a short vibration record. It shall be then kept in mind that the information on mutual modulation of the wheels is discarded.

2.1.3 Gear Condition Indicators

A common monitoring strategy in the industry is reducing the acquired vibration to a set of indicators which can represent the data in a compact way. In the literature, a number indicators were proposed and extensively tested for prompt detection specific damages in gear assets (see e.g. [27, 41, 42]). The health monitoring strategy is based on observing the deviation of such indicators from their nominal values, which are expected to be in some range usually estimated statistically. As already mentioned, signals acquired in different operating conditions and configurations will present a certain between-acquisitions variability, which is reflected directly in the CI values. Based on the analysis presented in 2.1.2, features related to a given gear can be extracted from the estimation $\hat{s_g}(t)$ of $s_g(t)$. A basic strategy for monitoring could be based on defining a similarity measure between the test signals and a reference expected signature. However, specifying the invariants for the measure under uncertain operating conditions effects is no trivial task. In the case under analysis, the CI computed as the second and fourth statistical moments of $\hat{s}_g(t)$ were considered for condensating the information contained in $\hat{s}_g(t)$ instead. The extraction of scalar CI from vibration records has the advantage of providing a meaningful way of condensating information and a quick analysis tool. It was observed on operational data that the extracted CI present a joint distribution showing some degree of correlation, linked to the operational (latent) variables. Specifically, the second and fourth statistical moments were selected in this work for characterizing the signal due to their ability of keeping track of the global changes in the signal distribution, although in general they are not suitable for differential diagnosis leading to discrimination between different gear fault types. Several more specific indicators were considered, such as modulation amplitude around the gearmesh (MOD), amplitude of shaft/mesh harmonics (OM), narrowband energy of the signal (NBE) or high order gearmesh sidebands connected to frequency modulation. Indicators designed ad-hoc for the detection of a specific fault should in general perform better in the detection task of such a fault. However, it is in the scope of the proposed methodology to devise an anomaly detection procedure relying on minimal assumptions on the nature of the mechanical fault that could arise, being robust to the unknown effects of the changing operational conditions of the monitored helicopters, and finally reducing the number of indicators that necessitate to be monitored. The afore-mentioned specific indicators span a wide set of features connected to specific degradations and are prone to result into noisy features when different faults arise (see Section 3.2.3). Therefore, it was preferred to obtain a minimal set of global statistics (second and fourth statistical moments of the extracted gear signal) which are more likely to be influenced by any change of the mechanical state of the component. Further, by considering a joint description of the features, the operational conditions influence is kept into account, enabling the methodology to differentiate properly between changes due to operating conditions and changes due to mechanical degradation. It should be however kept in mind that the proposed methodology is general and applies for any set of descriptors of the signal of interest (SOI) showing a correlation structure through the helicopter operating state. Due to the finite length of the records, the selected statistical moments are estimated from the discrete signals. The resulting CI are taken as the square root of the variance, for it represents the Root Mean Square (RMS) value of the zero-mean signal and is commonly employed in the industry, and the standardized fourth statistical moment (Kurtosis) as follows:

1. Root Mean Square value of the discrete signal (RMS)

$$RMS = \\ = \sqrt{\frac{1}{N_s} \sum_{k=1}^{N_s} (x_{SA}(k\Delta\phi)) - \bar{x}_{SA})^2} \tag{10}$$

2. Kurtosis of the discrete signal (KRT)

$$KRT = \frac{\sum_{k=1}^{N_s} (x_{SA}(k\Delta\phi) - \bar{x}_{SA})^4}{N_s RMS^4}, \tag{11}$$

where k indicates the sample number, $\Delta\phi$ the samples spacing in the angular domain, N_s the number of samples and $\bar{x}_{SA}$ the mean value of the shaft-synchronous signal samples. Considering those indicators provides a set of two CI that are able of describing the global properties of the gear signal, which are likely to change in a faulty state.

2.2. Support Vector Data Description

SVDD is a data domain description method inspired by the support vector machines ([43–45]). The basic idea is to determine, from a small set of training samples, the minimal volume hypersphere enclosing most of the target data. New instances outside the boundaries of the describing hypersphere are then classified as outliers. SVDD is suitable for the problem of fault detection when fault data are not available, since it only requires normal (target) objects in order to find a description of the normal state. The problem can be cast as a standard quadratic optimization with unique optimal solution ([46]), resulting in high computational efficiency for the method. In the following, the SVDD method as reported in [13] is briefly introduced. Assume a training set composed of M objects $\{\mathbf{x}_i, i = 1, 2, ..., M\}$ which are drawn from the target distribution. Being $\mathbf{a}$ the center of the hypersphere and R its radius, the cost function to be minimised reads:

$$F(R, \mathbf{a}) = R^2, \tag{12}$$

subject to the constraints:

$$||\mathbf{x}_i - \mathbf{a}||^2 \leq R^2, \qquad \forall i. \tag{13}$$

Cost function (12) is modified as to allow the possibility to reject some training points from the description, introducing slack variables $\xi_i \geq 0$ such that large distances from the center $\mathbf{a}$ are penalised:

$$F(R, \mathbf{a}) = R^2 + C\sum_i \xi_i. \tag{14}$$

Constraints (13) hence become:

$$||\mathbf{x}_i - \mathbf{a}||^2 \leq R^2 + \xi_i, \qquad \xi_i \geq 0, \qquad \forall i. \tag{15}$$

The parameter C controls here the trade-off between the volume of the hypersphere and the errors. Incorporating the constraints (15) into equation (14) by using Lagrange multipliers $\alpha_i \geq 0$ and $\gamma_i \geq 0$ leads to:

$$\begin{aligned} L(R, \mathbf{a}, \alpha_i, \gamma_i, \xi_i) = \\ = R^2 + C\sum_i \xi_i - \sum_i \alpha_i \{R^2 + \\ + \xi_i - [\|\mathbf{x_i}\|^2 - 2(\mathbf{a} \cdot \mathbf{x}_i) + \\ + \|\mathbf{a}\|^2]\} - \sum_i \gamma_i \xi_i. \end{aligned} \tag{16}$$

In (16), L should be minimised with respect to $R, \mathbf{a}, \xi_i$ and maximised with respect to the Lagrange multipliers α_i and γ_i. Setting to zero the partial derivatives gives the constraints:

$$\frac{\partial L}{\partial R} = 0 : \qquad \sum_i \alpha_i = 1 \tag{17}$$

$$\frac{\partial L}{\partial \mathbf{a}} = 0 : \qquad \mathbf{a} = \sum_i \alpha_i \mathbf{x}_i \tag{18}$$

$$\frac{\partial L}{\partial \xi_i} = 0 : \qquad C - \alpha_i - \gamma_i = 0. \tag{19}$$

From (19) and from the Lagrange multipliers being non-negative, the γ_i can be removed by imposing:

$$0 \leq \alpha_i \leq C. \tag{20}$$

Substituting back (17)–(19) into (16) results in:

$$L = \sum_i \alpha_i (\mathbf{x}_i \cdot \mathbf{x}_i) - \sum_{i,j} \alpha_i \alpha_j (\mathbf{x}_i \cdot \mathbf{x}_j), \tag{21}$$

subject to the constraints (20). Now when a training object $\mathbf{x}_i$ strictly satisfies the inequality in (15), the constraint is satisfied and the corresponding α_i is zero. Differently, when (15) holds with equality, the constraint has to be enforced ($\alpha_i > 0$). Hence:

$$||\mathbf{x}_i - \mathbf{a}||^2 < R^2 \rightarrow \alpha_i = 0, \gamma_i = 0 \tag{22}$$

$$||\mathbf{x}_i - \mathbf{a}||^2 = R^2 \rightarrow 0 < \alpha_i < C, \gamma_i = 0 \tag{23}$$

$$||\mathbf{x}_i - \mathbf{a}||^2 > R^2 \rightarrow \alpha_i = C, \gamma_i > 0. \tag{24}$$

From equation (18), the center of the sphere is a linear combination of the objects, hence only training objects for which $\alpha_i > 0$ are needed for the description and they are therefore named support vectors (SV's) of the description. Besides, support vectors lie on the boundary of the hypersphere, hence R^2 can be obtained as the distance from any support vector to the center of the hypersphere $\mathbf{a}$. The distance of any new object $\mathbf{z}$ from the center of the hypersphere is then

computed as:

$$\begin{aligned}\Delta(\mathbf{z}) &= \|\mathbf{z}-\mathbf{a}\|^2 = \\ &= (\mathbf{z}\cdot\mathbf{z}) - 2\sum_i \alpha_i(\mathbf{z}\cdot\mathbf{x}_i) + \\ &+ \sum_{i,j}\alpha_i\alpha_j(\mathbf{x}_i\cdot\mathbf{x}_j).\end{aligned} \tag{25}$$

In order to allow for more flexible boundaries (i.e. when data do not follow a spherical distribution), the inner product $(\mathbf{x}_i \cdot \mathbf{x}_j)$ can be replaced by a kernel function $K(\mathbf{x}_i, \mathbf{x}_j)$ satisfying Mercer's theorem ([16]). In this way, the input space is implicitly mapped to some other high-dimensional feature space, where the data are better described from the hypersphere. Equation (25) reads then in the new feature space:

$$\begin{aligned}\Delta(\mathbf{z}) &= K(\mathbf{z},\mathbf{z}) - 2\sum_i \alpha_i K(\mathbf{z},\mathbf{x}_i) \\ &+ \sum_{i,j}\alpha_i\alpha_j K(\mathbf{x}_i,\mathbf{x}_j).\end{aligned} \tag{26}$$

A common choice for the kernel function is the Gaussian kernel, defined as:

$$K(\mathbf{x}_i,\mathbf{x}_j) = \exp\left(\frac{-\|\mathbf{x}_i-\mathbf{x}_j\|^2}{\sigma^2}\right), \tag{27}$$

where σ is the (positive) width parameter of the Gaussian kernel: smaller values result in a tighter solution with lower generalization ability, characterized by the presence of more support vectors, whereas higher values result in a more flexible description of the data set. It can be shown that in the limit for small σ, the solution of the optimization problem (16) is such that all objects become support vectors and coincides with Parzen density estimation with a small kernel width. On the other hand, very large values approximate the initial spherically shaped solution ([13]). This kernel is independent of the position of the dataset with respect to the origin, i.e. only the distance between objects matters. Objects are mapped to unit norm vectors, so that only the angles between them count ([13]). In the standard SVDD setting, objects are rejected and flagged as outliers when they lie outside the hypersphere ($\Delta > R^2$). Optimal selection of the model parameters (C and σ) is still an open issue in data description problems. In this article, the approach proposed by Tax in [47] is used. Such an approach consists of generating an artificial outlier class (uniformly distributed N-sphere around the training data, where N is the dimension of the set of features) in order to estimate the volume of the classifier. The optimal description parameters are found by minimizing the cost function:

$$E(\sigma, C) = \lambda\left(\frac{N_{SV}}{N_{train}}\right) + (1-\lambda)(1-POD), \tag{28}$$

where λ is introduced in order to adjust the trade-off between the importance of false alarms and probability of detection and is here set as $\lambda = 0.5$ in order to give equal weight to both. The quantity N_{SV}/N_{train} is the ratio between the number of support vectors in the model (dependency on model parameters omitted in the notation) and the number of training points and provides a Leave One Out (LOO) estimate of the probability of false alarm, whereas the probability of detection is estimated from the artificial outlier class. The quantity $(1 - POD)$ can indeed be interpreted as a Montecarlo estimate of the volume of the classifier, owing to the uniform distribution of the introduced outliers, it is as well depending on the model parameters. Furthermore, the quantity $\nu = 1/CN_{train}$ upper-bounds the error on the target set (i.e. the probability of false alarm), hence it is possible to set C accordingly, thus optimizing (28) with respect to σ only.

2.3. Proposed methodology

Because the variation in the operating conditions of the machine affects the CI values through the influence on the measured response as from equation (1), CI values are expected to be correlated to the operating condition parameters. Studies on the correlation among different CI and between CIs and operating conditions are reported in [9], highlighting strongly non-linear correlation. Ideally, such a correlation would change with mechanical degradation progressively affecting the measured response signal. Therefore, it is proposed to extend the idea described in [11] of fusing multiple CI in an AS (therein referred to as Health Indicator), keeping into account the non-linearities in the correlation between indicators induced from the underlying unknown operating variables. The idea behind the AS is then to exploit the correlation information in order to obtain better separation between the healthy state and the faulty state of a given component, under the assumption that given a sufficient amount of observations, vibration data will be acquired under similar conditions for a helicopter operating similar mission profiles, i.e. assuming that a sufficient number of vibration acquisitions is representative of the baseline vibration behavior. In order to retain the non-linearities in the CI correlation model, a SVDD model for the healthy distribution is proposed instead of a multivariate Gaussian one. The metric for the AS was selected

to be the distance of an observation from the center of the hyper-sphere in the kernel space, according to equation (26). The metric of the AS for the Gaussian model was computed as the squared Mahalanobis Distance ([48]) of an observation to the learnt Gaussian model, according to [11]. The algorithm involves a learning phase, in which models are trained using N_{train} observations, and an evaluation phase in which new observations are compared to the model and an AS obtained. All considered features are normalized by z-score during the learning phase in order to obtain meaningful descriptions. The learning phase can be triggered from the operator after any relevant maintenance action, manually entered or automatically detected with methods like, e.g., the one mentioned in [11]. The issue of setting a threshold on the AS values in order to decide whether an observation is normal or not is not addressed in this work, since it involves several additional steps which are part of the overlying logic (see Figure 1). Seemingly, N_{train} needs to be determined according to the maintenance policy and is given here as a constraint.

3. Experimental results

3.1. Preliminary data characterization

Flight data have been recorded from two piezoelectric accelerometers mounted on the gearbox case of a H135 helicopter. The monitoring system with which the considered helicopter was equipped recorded the output acceleration from seven sensors at different locations. Three of them are dedicated to monitoring the cabin vibration, one to the tail drive shaft, one to the tail gearbox and the latter two to the main gearbox. A sketch of the main gearbox is shown in Figure 2. The two input drive shafts rotate at a speed of about 98.3Hz (≈5900rpm) and transmit power from the engines to the main gearbox. Shafts speed ranges from about 6.5Hz at the main hub shaft to 210Hz at the fan drive shaft at 100% nominal engine speed. The main gearbox accelerometers are located on the right and left side of the case, in proximity of the input drive shafts and measure the radial acceleration. For monitoring purposes, the system periodically acquires around 2.85s of vibration data per acquisition per accelerometer. The system starts recording only when flight conditions are stable (contextual correction in Figure 1), as to prevent from acquiring highly non-stationary vibration data (e.g. during start-up), restricting in a first place the space of possible occurring operating conditions during a record. A first effect of the constraint is reducing the number of acquisitions in a given period, the second is that of imposing a first limitation to the CI values variability due to the different operating conditions. Additionally, due to memory constraints from the acquisition system, a maximum number of files is stored during each flight session. Together with vibration, a magnetic pickup installed on the main rotor swash plate and one on the tail rotor store a synchronizing signal, allowing for the establishment of angle/time relationships used for resampling of the TSA signal. The mechanical complexity of the system and the flight environment results in multiple vibration sources, mainly consisting of main rotor and blades vibration, wind/structure interactions and other aerodynamic effects and vibration directly related to the rotating components, like unbalanced/misaligned shafts or meshing gears. The mixture of all these sources is transmitted through the structure to the accelerometers according to model (1), giving rise to a profuse spectrum in which characteristic frequencies are hardly identifiable. A typical measured spectrum in a fault-free condition is shown in Figure 3. The peak of the response at about 2260Hz is the meshing frequency of the input drive gear and the intermediate shaft output pinion. Such a noisy spectrum justifies the introduction of signal processing techniques, based on a first-principle understanding of the effect that the developing damage has on the measured vibration signal (section 2.1.2). The data used for this analysis were acquired during almost 22 months of operating life of the helicopter (≈2130 Flight Hours). In this time frame, micro-pitting degradation occurred on the right input drive shaft's pinion. Ground truth is available from two inspections carried on after 1600 FH and 2130 FH. After the first inspection, the measured damaged area was about 16mm^2 and was judged safe for the operations of the gears. The damaged area at the time of the second inspection was about 34mm^2 and the asset was then replaced. The degradation is visible in the form of gray staining on the tooth surface (Figure 4). The damage started developing between 1000 FH and the date of first assessment. However, no feedback on direct inspections of the component is available before the 1600 FH inspection.

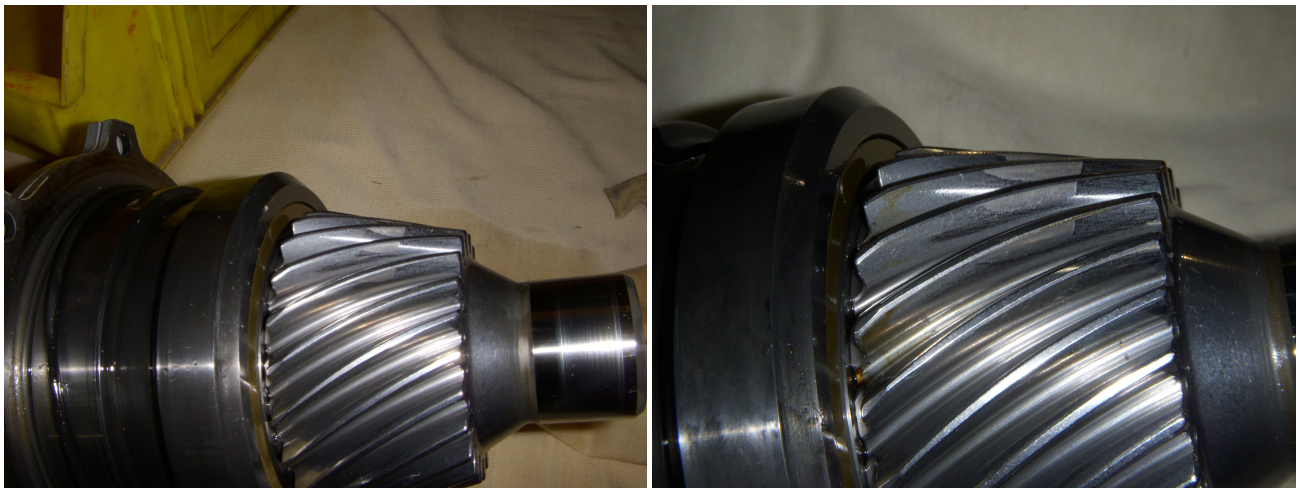

(a) (b)

Figure 4: Gray staining on the right input drive shaft's pinion. a) Component at the time of first inspection; b) component at the time of second inspection.

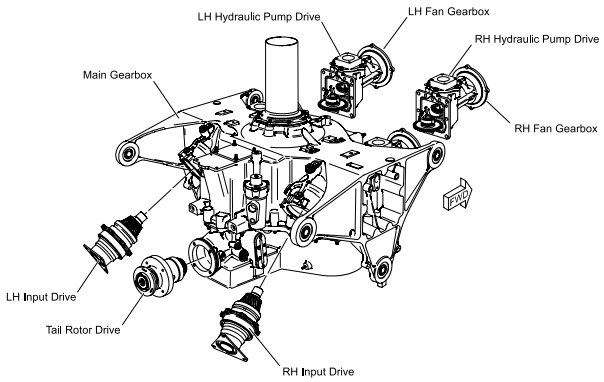

Figure 2: H135 main gearbox.

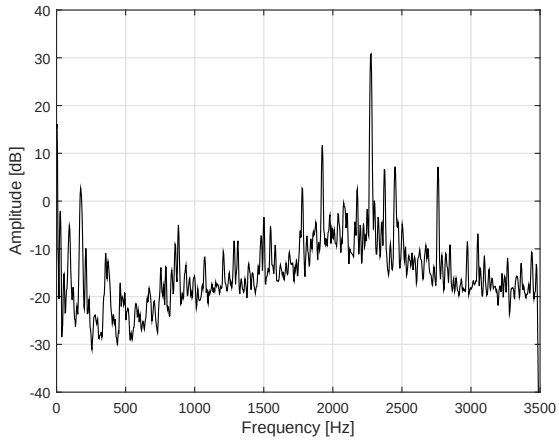

Figure 3: Spectrum of a 2.85s fault-free vibration signal recorded in flight by one of the monitoring system main gearbox accelerometer with a sampling frequency of 7000Hz (estimated using Hanning window and 16 non-overlapping averages).

3.2. Fault detection performance

For verification purposes, and with reference to the previously reported maintenance inspections, the flight data were divided in the following sequential blocks:

1. Healthy state (≈1000 FH);
2. Early degradation (unknown state) (≈600 FH);
3. Known degradation (faulty state) (≈530 FH).

The proposed methodology, based on AS generation through SVDD data fusion is assessed by comparing its performance in detecting the early degradation with respect to the univariate analysis of the CI proposed in section 2.1 and with respect to the method based on the Gaussian model proposed in [11]. First, the CI computed over the entire data history are presented. Next, the Gaussian and the proposed method are applied using $N_{train} = 80$ acquisitions for training and the remaining for evaluation of the AS. Since the goodness of the obtained multivariate model depends on some extent on the representativeness of the training set, the models were trained picking all the possible training sets from the healthy data. In this way, robustness to eventually poorly representative training sets is accounted for. Classification performance can be measured independently from threshold setting by introducing the receiver operating characteristic (ROC) curves. Such curves represent the fraction of target objects accepted by the model (i.e. healthy observations classified as healthy) against the fraction of outliers accepted (i.e. faulty observations classified as healthy). The area under the ROC curve (AUC) gives a scalar measure of the

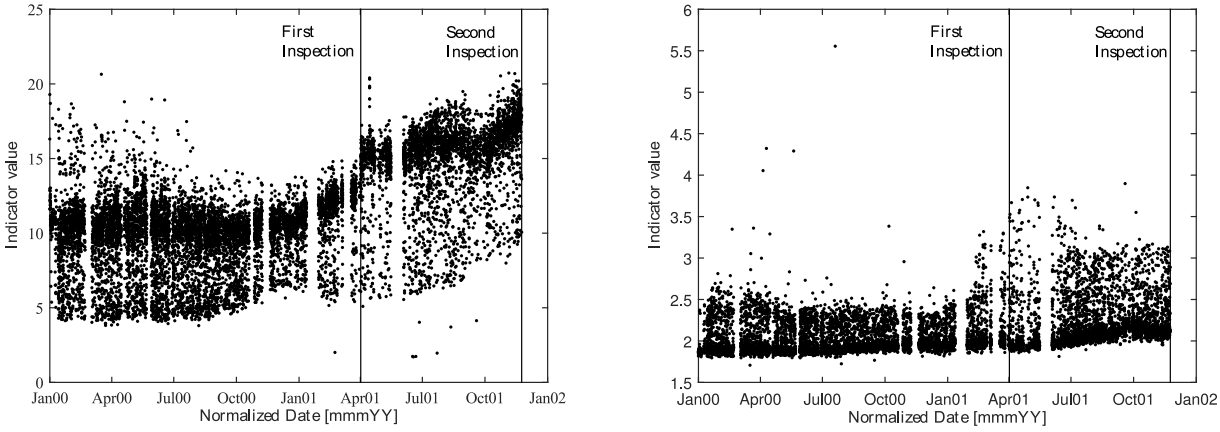

(a) **(b)**

Figure 5: Time history of the condition indicators (time axis is translated such that the first acquisition coincides with the reference date of 01 Jan 00). Black vertical lines: first inspection and second inspection. a) RMS CI; b) Kurtosis CI.

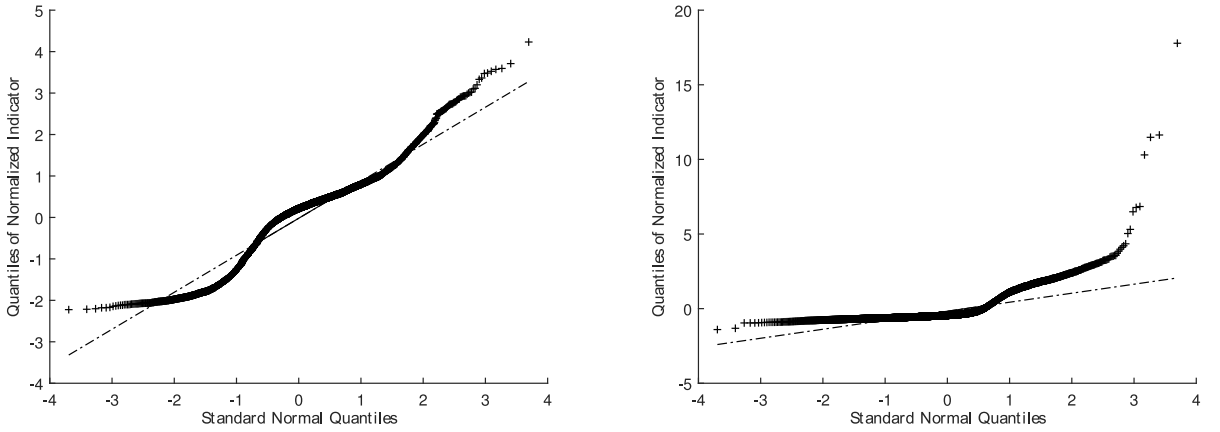

(a) **(b)**

Figure 6: Normality test of each CI visualized through quantile-quantile plots. a) RMS CI; b) Kurtosis CI.

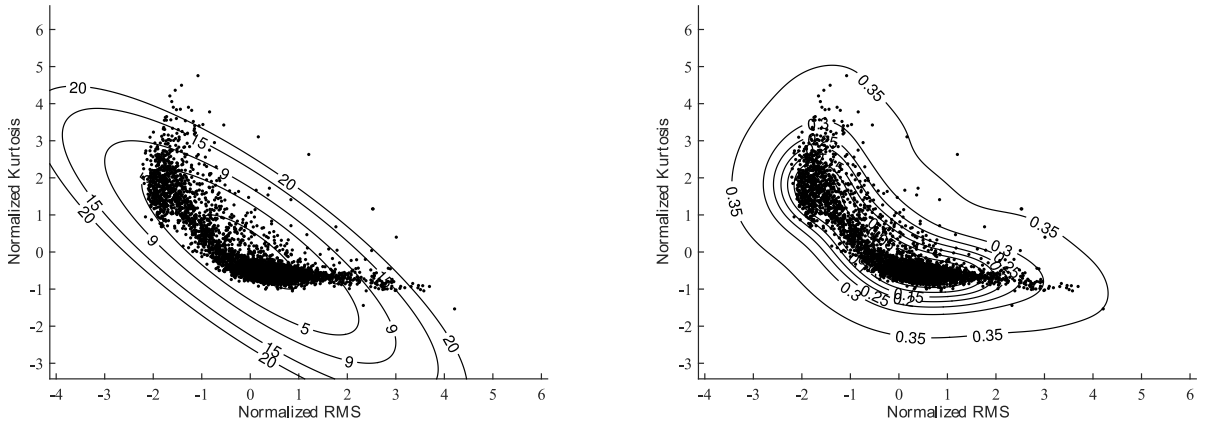

(a) **(b)**

Figure 7: Scatter plots of the CI in the normalized feature space and contours representing varying AS. a) Gaussian model contours; b) SVDD model contours.

achieved separability between states. Computing the classification performances requires the definition of a healthy and a faulty dataset. The healthy dataset was defined including the first 1000 FH, whereas four definitions are introduced for the faulty state: early stage degradation (from FH 1150); middle stage degradation (from FH 1300); advanced stage degradation (from FH 1450) and assessed degradation (from FH 1600). The models were evaluated in the four cases, which allows for comparing their efficiency in responding early to the fault development in terms of AUC, without introducing model-specific thresholds or novel key performance indexes. The CI extracted from the vibration data were computed as described in section 2.1. Figure 5 shows the values of the RMS and Kurtosis indicators computed from the shaft-synchronous signal. The dates in which damage was assessed are indicated with black vertical lines. Although there is a clear upward trend correlated with the degradation, the values are very scattered and present a complex distribution. A visualization of the CI distribution in the healthy state is shown in Figure 6, where the quantiles of the CI distributions are plotted against the quantiles of the normal distribution. It can be seen that both the CI distributions do not match the Gaussian (dashed line in the figure). In Figure 7, scatter plots of the CI centred in the feature space normalized by their mean are shown. The contours of example data descriptions obtained using the Gaussian model and the SVDD model are plotted for varying AS values. It is evident that the SVDD model produces a tighter description, which results in a better ability of discriminating between those data points belonging to the healthy distribution all the others not belonging to it.

3.2.1 Receiver Operating Characteristic curves and related measures

The ROC curves in the four degradation cases mentioned above are shown in Figure 8. The curves for the multivariate models are obtained as mean ROC curves over all the possible 4680 ROC curves computed on training sets obtained drawing a sequence of N_{train} acquisitions from the healthy distribution. The mean AUC, computed from the mean ROC curve, is reported in the legend along with the AUC values standard deviation in squared brackets. The indicators (both from the multivariate and from the univariate models) gain a better discriminating ability with the damage progression. This is not surprising, since the CI are designed for being correlated with fault evolution and hence their value increase with the defect growth. However, both the multivariate indicators performs better in general. Moreover, they offer the advantage of resuming the information from multiple CI in one single AS, thus enabling simpler decision. The AS computed from SVDD model is the one granting highest probabilities of detection at a given probability of false alarm in the early, middle and advanced degradation stages, whereas for more several degradation (first inspection onward), the Gaussian model performs slightly better on average, since the healthy and faulty distributions becomes very well separated in the features space. Except for the last stage, the SVDD model is more robust to the variability of the training set with respect to the Gaussian model, as observed from the standard deviation values. In order to better visualize the influence of different training sets, a boxplot of the AUC values in the four degradation stages is shown in Figure 9. Training sets which are more representatives of the real multivariate distribution of the indicators leads in general to higher AUC scores for the multivariate models. The horizontal black lines in the plot represent the AUC computed for the best-performing univariate CI, whereas the boxes represent the AUC values for different training sets obtained for the multivariate models. In general, the SVDD model results in higher AUC than the univariate models for almost all the possible training sets, yielding an AUC relatively close to that of the univariate CI in the few cases in which they perform better. The Gaussian model suffers more from the training set representativeness in the first three considered degradation stages. However, in the majority of the cases it yields better performance than the univariate indicators, outperforming also the SVDD model when considering the severe degradation case.

3.2.2 Methods comparison

Tables 1 to 4 summarize the comparison between SVDD AS and Gaussian AS for the four considered degradation cases, by the mean of three parameters. The first one is the average AUC gain (AAG), defined as the difference between the mean AUC value obtained over all the training sets and the best AUC value from the univariate CI. The second parameter is the failure rate (FR), defined as the count of the cases in which the multivariate model performed worst than the best univariate CI divided by the total number of cases (4680). The third introduced parameter is the worst AUC loss (WAL), defined as the difference between the best AUC from the univariate CI and the worst case AUC valued obtained for the AS. From the tables, the AS from SVDD model outperforms both the AS from Gaussian model and the univariate CI for early detection. Once the fault condition is sufficiently developed, it seems that the Gaussian model performs slightly better with respect to the

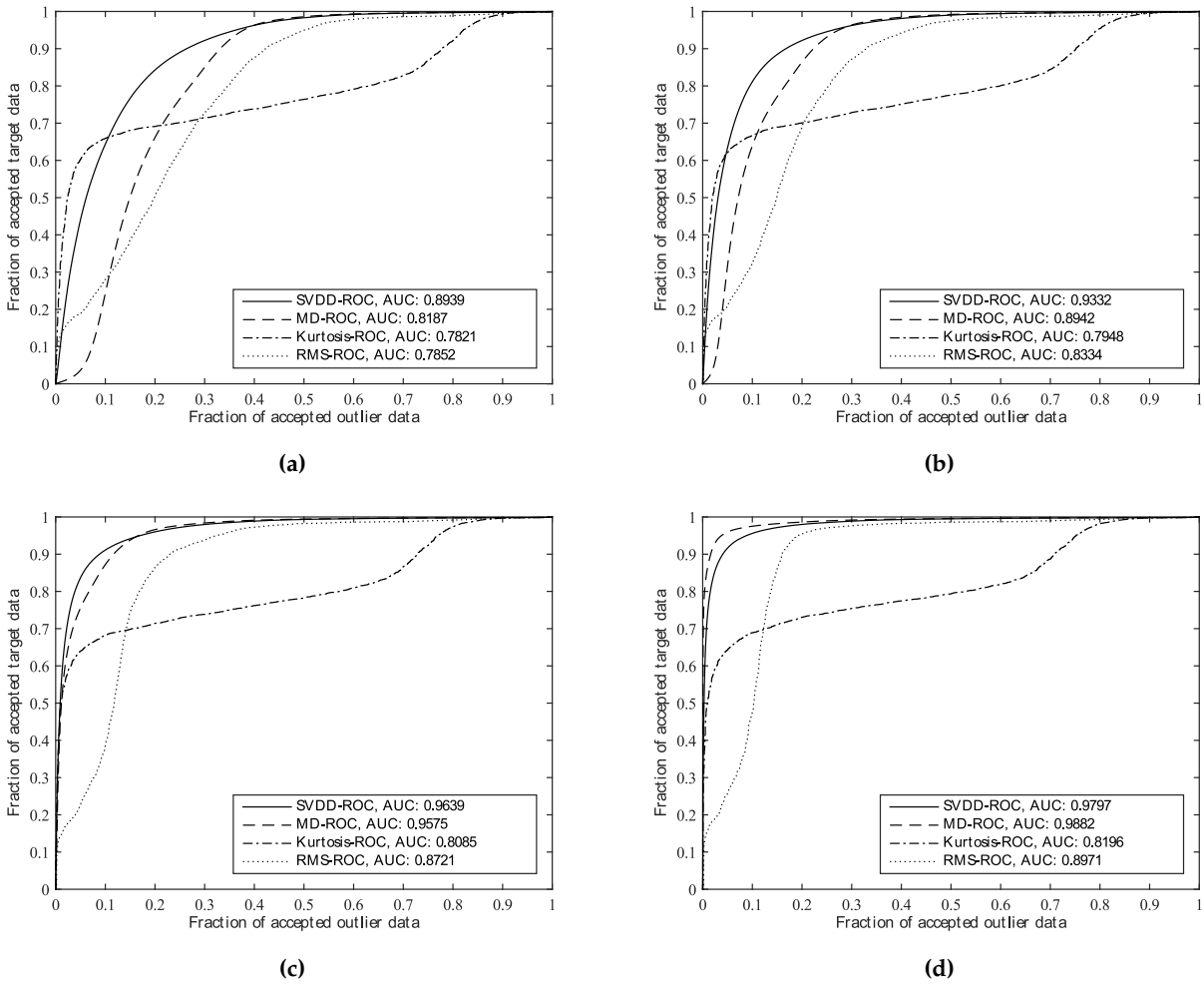

Figure 8: ROC curves. SVDD and Gaussian model average performance over 4680 training sets compared with univariate CI performance in the four degradation stages. a) Early stage degradation; b) middle stage degradation; c) advanced stage degradation and d) minimum assessed micro-pitting of 16mm^2

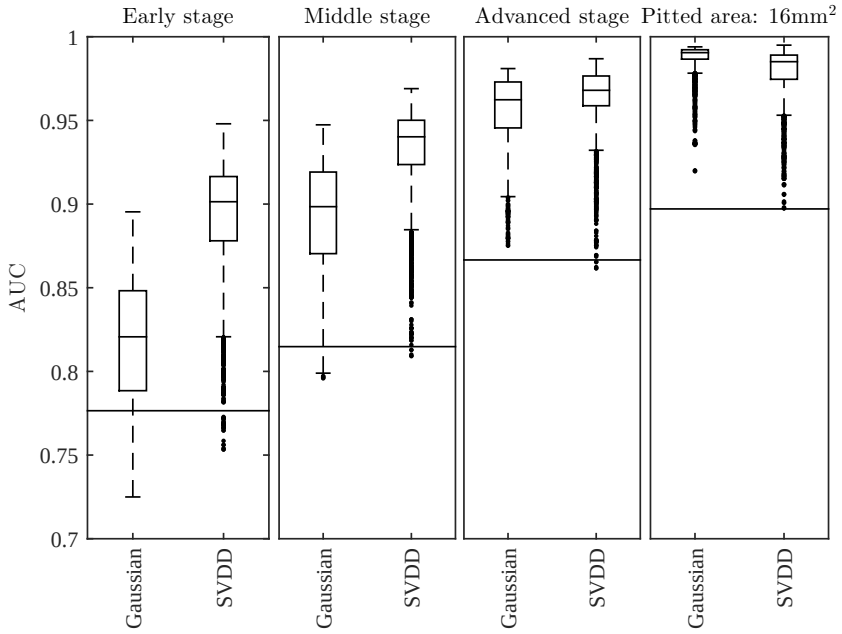

Figure 9: Boxplot of AUC values obtained in the four degradation cases for the Gaussian and SVDD models over the 4680 evaluations, compared to the AUC of the best performing CI (black lines in the plot).

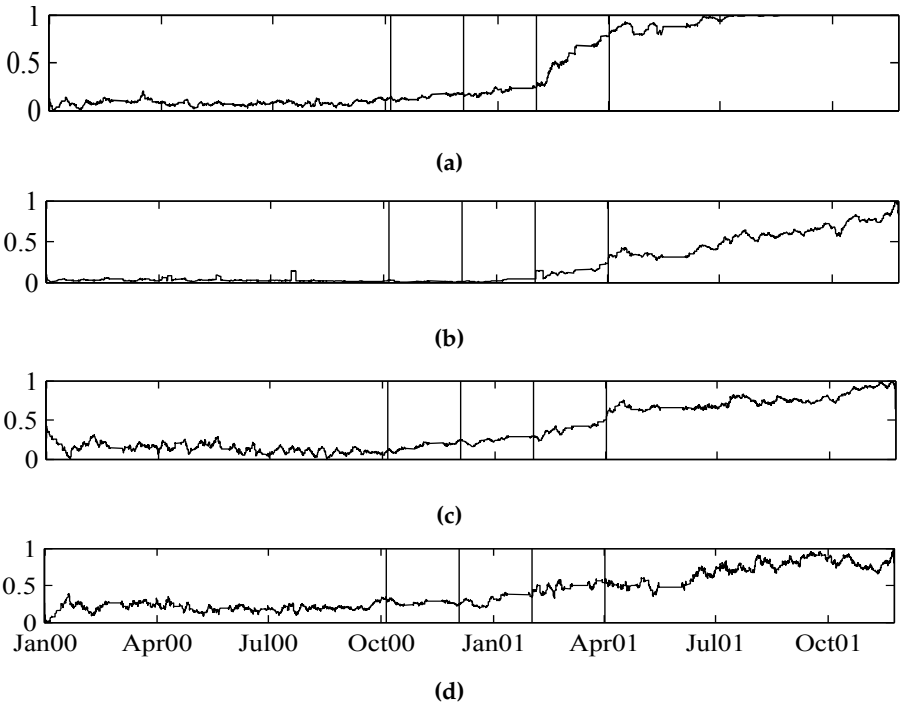

Figure 10: Trend values of the AS and the CI computed using a moving average filter with a length of 100 acquisitions. The vertical black lines indicate the defined damage stages (time axis is translated such that the first acquisition coincides with a reference date of 01 Jan 00). a) SVDD AS; b) Gaussian AS; c) RMS; d) Kurtosis.

SVDD, owing to the increased topological separation between the cluster of the anomalous points and that of the reference distribution in the CI space. However, both the multivariate models consistently outperform the traditional univariate CI analysis. These results translate into a clearer ability of the AS of reacting to the faults with respect to the CI, as shown in Figure 10, where the AS and CI trends are compared. Trends are obtained using a moving average filter with a length of 100 acquisitions. The black vertical lines indicate the beginning of each of the four defined sequential degradation stages. It is observed that the AS from the SVDD model is reacting quicker to the fault initiation, resulting in improved fault detection ability. Having indicators which are able of better separating faulty states from the healthy ones is preferable, since using the same number of points, increased confidence in the decision can be obtained, whatever the decision policy is.

Table 1: Comparison of AS and CI performance, early stage degradation

Parameter	Gaussian model	SVDD model
AAG	0.0422	**0.1174**
FR	0.1558	**0.0064**
WAL	0.0515	**0.0232**

Table 2: Comparison of AS and CI performance, middle stage degradation

Parameter	Gaussian model	SVDD model
AAG	0.0794	**0.1184**
FR	0.0058	**0.0011**
WAL	0.019	**0.0056**

Table 3: Comparison of AS and CI performance, advanced stage degradation

Parameter	Gaussian model	SVDD model
AAG	0.0909	**0.0973**
FR	**0**	0.0011
WAL	**-**	0.005

Table 4: Comparison of AS and CI performance, minimum assessed micro-pitted area of $16mm^2$

Parameter	Gaussian model	SVDD model
AAG	**0.1216**	0.1131
FR	0	0
WAL	-	-

3.2.3 Influence of feature selection

Features (or CI) for defining an AS should be selected such as to capture global changes of the signal of interest, so that increasing values of the AS, triggering a departure of the signature from baseline, are representative of a change of the dynamic properties of the component under analysis. However, one may include specific CI in the signal description in order to design an AS reacting more promptly to a known fault. With illustrative purpose, in this section the previous analysis is repeated on an expanded gear AS defined as the combination of four CI. Namely, the OM1 and OM2, amplitude of the first and second harmonics of the reference shaft SA signal, are additionally included in the previous description. In this way, the AS additionally includes two CI typically related to shaft unbalance and misalignment. Due to the fact that the considered fault case does not involve shaft unbalance/misalignment, both the added CI are insensitive to the changes provoked by the fault. Moreover, such CI are not describing the global properties of the signal of interest, but specific features of its frequency (order) domain representation. The boxplot of the AUC scores is presented in Figure 11 in the same fashion of Figure 9. Although the AS keep performing better than the univariate CI, an average decrease in performance is observed. In an anomaly detection framework, this can be explained as increasing the ratio of irrelevant features in the descriptions leads in general to decreased performance of anomaly detection metrics (noise attributes problem in [49]). This fact can also be used for intuitively explaining why the noise attributes OM1 and OM2 are affecting less the performance of the Gaussian description than that of the SVDD model. In fact, the SVDD model is aimed to better capturing the intrinsic dimensionality of the data through accounting for a general correlation structure. As a consequence, it is less accurate when features hiding this correlation structure are introduced. On the countrary, the Gaussian description may only account for a linear correlation, and results therefore less influenced. In general, a well-defined AS shall then better consist of a set of CI which are able of capturing a global description of the signal of interest, rather than of a set of CI tailored for the detection of specific faults.

4. Conclusion

In this paper, an anomaly-detection procedure devoted to the quantification of the degree of deviation of the mechanical state of a component from its nominal condition is developed. The work reported on the possibility of obtaining improved information from

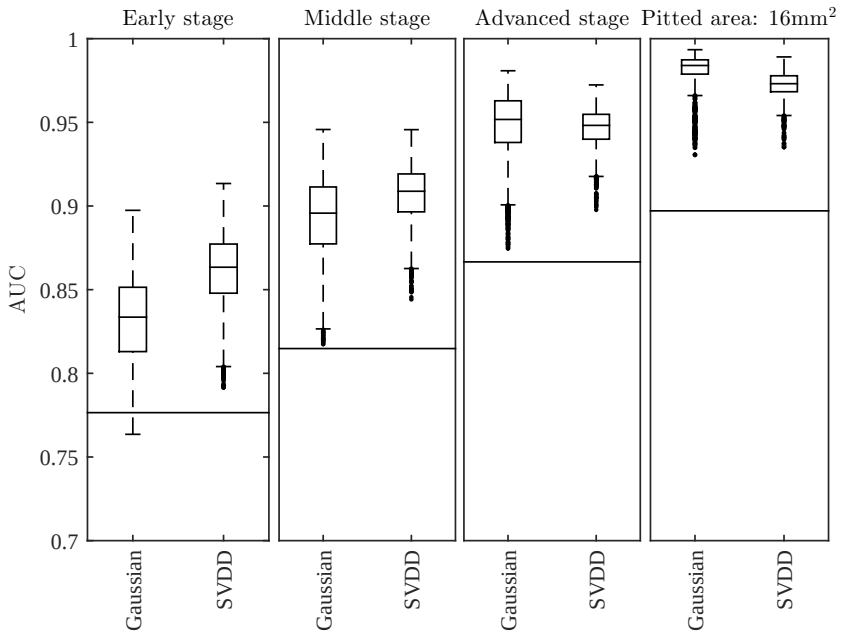

Figure 11: Boxplot of AUC values obtained in the four degradation cases for the Gaussian and SVDD models ($\mathbb{R}^4$ features set) over the 4680 evaluations, compared to the AUC of the best performing CI (black lines in the plot).

Health and Usage Monitoring Systems vibration data by fusing traditional CI into a single AS using data description models. Such an improvement is achieved by considering the variability induced by the operating conditions of the helicopter on the CI values implicitly inside the AS models, in the form of a correlation between multiple CI through latent variables. The models are learnt from the acquired data during a learning phase of the algorithm. Therefore, a set of reference values are needed before the monitoring can be effectively enabled. Remarkably, since operating conditions are treated as latent variables, there is no need for direct measurements of the flight parameters. In order to address the limits of the original proposal based on a Gaussian model, an SVDD model was introduced. The method allowed to obtain an AS which improved the detection of early stage degradation with respect to the AS obtained from the Gaussian model and with respect to traditional univariate CI. Moreover, only few training acquisitions were sufficient for learning a proper data description. The choice of the model parameters was automatized, yielding good results for the considered case. The method was assessed on comprehensive real operating vibration data. It was shown that although the multivariate models depend on some extent on the training set representativeness of the true distribution, reasonably robust performance improvements could be obtained over the univariate CI. However, no general indication can be given on the minimum number of the training acquisitions necessary for an accurate description of a set of CI, which greatly depends on the characteristics of the distribution. The selection of CI for building proper AS in the anomaly detection framework was discussed, and the effect of adding insensitive CI considered. Importantly, it was highlighted that due to the very nature of the anomaly detection problem, the CI used for building a valid AS shall be able of capturing globally the nominal behavior of the signal of interest, rather than reacting to each possible fault, a fact often overlooked in previous works on the subject.

References

[1] Anthony RS Bramwell, David Balmford and George Done. *Bramwell's helicopter dynamics*. Butterworth-Heinemann, 2001.

[2] U.S. Army. *ADS-79C-HDBK, Aeronautical Design Standard: Handbook for Condition Based Maintenance Systems for US Army Aircraft Systems*. 2012.

[3] Abdel Bayoumi et al. "Conditioned-Based Maintenance at USC-Part I: Integration of Maintenance Management Systems and Health Monitoring Systems through Historical Data Investigation". In: *Proceedings of the AHS International Specialists Meeting on Condition Based Maintenance, Huntsville, AL*. 2008.

[4] Brian D Larder, Mark W Davis and CT Stratford. "HUMS Condition Based Maintenance Credit Validation". In: *American Helicopter Society 63rd Annual Forum*. 2007.

[5] Johan Wiig. "Optimization of fault diagnosis in helicopter health and usage monitoring sys-

tems". PhD thesis. Aix-en-Provence, ENSAM, 2006.

[6] Venkat Venkatasubramanian et al. "A review of process fault detection and diagnosis: Part I: Quantitative model-based methods". In: *Computers & chemical engineering* 27.3 (2003), pp. 293–311.

[7] Paula J Dempsey, David G Lewicki and Dy D Le. "Investigation of current methods to identify helicopter gear health". In: *Aerospace Conference, 2007 IEEE*. IEEE. 2007, pp. 1–13.

[8] Akm Anwarul Islam et al. *Characterization and comparison of vibration transfer paths in a helicopter gearbox and a fixture mounted gearbox*. Tech. rep. TM-216586. NASA, 2014.

[9] Marianne Mosher, Edward M Huff and Eric Barszcz. "Analysis of in-flight measurements from helicopter transmissions". In: *American Heliopter Society 60th Annual Forum, Baltimore*. 2004.

[10] *Intelligent management of helicopter vibration health monitoring data: Based on a report prepared for the CAA by GE Aviation Systems Limited*. Vol. 2011/01. CAA paper. Norwich: Published by TSO on behalf of UK Civil Aviation Authority, 2012. ISBN: 9780117924031.

[11] S Bendisch and J Mouterde. "New methodologies to improve health and usage monitoring system (HUMS) performance using anomaly detection applied on helicopter vibration data". In: *39th European Rotorcraft Forum, Moscow*. 2013.

[12] Georg Wurzel. "Development of a Condition-Based Maintenance Concept for Helicopter Drive Systems". PhD thesis. Vienna University of Technology, 2011.

[13] David MJ Tax and Robert PW Duin. "Support vector data description". In: *Machine learning* 54.1 (2004), pp. 45–66.

[14] Zhiqiang Ge, Furong Gao and Zhihuan Song. "Batch process monitoring based on support vector data description method". In: *Journal of Process Control* 21.6 (2011), pp. 949–959.

[15] Sang-Woong Lee, Jooyoung Park and Seong-Whan Lee. "Low resolution face recognition based on support vector data description". In: *Pattern Recognition* 39.9 (2006), pp. 1809–1812.

[16] David MJ Tax and Robert PW Duin. "Support vector domain description". In: *Pattern recognition letters* 20.11 (1999), pp. 1191–1199.

[17] Carolina Sanchez-Hernandez, Doreen S Boyd and Giles M Foody. "Mapping specific habitats from remotely sensed imagery: support vector machine and support vector data description based classification of coastal saltmarsh habitats". In: *Ecological informatics* 2.2 (2007), pp. 83–88.

[18] D Tax, Alexander Ypma and R Duin. "Support vector data description applied to machine vibration analysis". In: *Proc. 5th Annual Conference of the Advanced School for Computing and Imaging (Heijen, NL)*. Citeseer. 1999, pp. 398–405.

[19] Yuna Pan, Jin Chen and Lei Guo. "Robust bearing performance degradation assessment method based on improved wavelet packet–support vector data description". In: *Mechanical Systems and Signal Processing* 23.3 (2009), pp. 669–681.

[20] Alexander Ypma, David MJ Tax and Robert PW Duin. "Robust machine fault detection with independent component analysis and support vector data description". In: *Neural Networks for Signal Processing IX, 1999. Proceedings of the 1999 IEEE Signal Processing Society Workshop.* IEEE. 1999, pp. 67–76.

[21] Dong Wang et al. "Support vector data description for fusion of multiple health indicators for enhancing gearbox fault diagnosis and prognosis". In: *Measurement Science and Technology* 22.2 (2010), p. 025102.

[22] Alexander Ypma and Robert PW Duin. "Support objects for domain approximation". In: ICANN. 1998.

[23] Edwin M Knorr, T. NG Raymond and Vladimir Tucakov. "Distance-based outliers: algorithms and applications". In: *The VLDB Journal* 8.3-4 (2000), pp. 237–253.

[24] David Martinus Johannes Tax. "One-class classification". In: (2001).

[25] Shehroz S Khan and Michael G Madden. "One-class classification: taxonomy of study and review of techniques". In: *The Knowledge Engineering Review* 29.3 (2014), pp. 345–374.

[26] WJ Wang and PD McFadden. "Early detection of gear failure by vibration analysis i. calculation of the time-frequency distribution". In: *Mechanical Systems and Signal Processing* 7.3 (1993), pp. 193–203.

[27] B David Forrester. "Advanced vibration analysis techniques for fault detection and diagnosis in geared transmission systems". PhD thesis. 1996.

[28] G Dalpiaz, A Rivola and R Rubini. "Effectiveness and sensitivity of vibration processing techniques for local fault detection in gears". In: *Mechanical Systems and Signal Processing* 14.3 (2000), pp. 387–412.

[29] CJ Stander, PS Heyns and W Schoombie. "Using vibration monitoring for local fault detection on gears operating under fluctuating load conditions". In: *Mechanical Systems and Signal Processing* 16.6 (2002), pp. 1005–1024.

[30] N Baydar and Andrew Ball. "Detection of gear failures via vibration and acoustic signals using wavelet transform". In: *Mechanical Systems and Signal Processing* 17.4 (2003), pp. 787–804.

[31] F Combet and L Gelman. "Optimal filtering of gear signals for early damage detection based on the spectral kurtosis". In: *Mechanical Systems and Signal Processing* 23.3 (2009), pp. 652–668.

[32] Jérôme Antoni. "The spectral kurtosis: a useful tool for characterising non-stationary signals". In: *Mechanical Systems and Signal Processing* 20.2 (2006), pp. 282–307.

[33] Jérôme Antoni and RB Randall. "The spectral kurtosis: application to the vibratory surveillance and diagnostics of rotating machines". In: *Mechanical Systems and Signal Processing* 20.2 (2006), pp. 308–331.

[34] Alexander Ypma. “Learning methods for machine vibration analysis and health monitoring”. PhD thesis. 2001.

[35] Victor Girondin et al. “Bearings fault detection in helicopters using frequency readjustment and cyclostationary analysis”. In: *Mechanical Systems and Signal Processing* 38.2 (2013), pp. 499–514.

[36] Jérôme Antoni et al. “Cyclostationary modelling of rotating machine vibration signals”. In: *Mechanical systems and signal processing* 18.6 (2004), pp. 1285–1314.

[37] David Abboud et al. “Envelope analysis of rotating machine vibrations in variable speed conditions: A comprehensive treatment”. In: *Mechanical Systems and Signal Processing* 84 (2017), pp. 200–226.

[38] Yunzhe Yang et al. “Detecting changes in gear surface roughness using vibration signals”. In: *Acoustics 2015, Hunter Valley, Australia*. 2015.

[39] KR Fyfe and EDS Munck. “Analysis of computed order tracking”. In: *Mechanical Systems and Signal Processing* 11.2 (1997), pp. 187–205.

[40] Francois Combet and Leonid Gelman. “An automated methodology for performing time synchronous averaging of a gearbox signal without speed sensor”. In: *Mechanical systems and signal processing* 21.6 (2007), pp. 2590–2606.

[41] David Siegel, Jay Lee and Paula Dempsey. “Investigation and Evaluation of Condition Indicators, Variable Selection, and Health Indication Methods and Algorithms For Rotorcraft Gear Components”. In: *MFPT 2014 Conference, Virginia Beach, VA*. 2014.

[42] Amani Raad, Jérôme Antoni and Ménad Sidahmed. “Indicators of cyclostationarity: Theory and application to gear fault monitoring”. In: *Mechanical Systems and Signal Processing* 22.3 (2008), pp. 574–587.

[43] Vladimir Vapnik, Steven E Golowich and Alex Smola. “Support vector method for function approximation, regression estimation, and signal processing”. In: *Advances in neural information processing systems 9*. Citeseer. 1996.

[44] Bernhard Scholkopf. “Support Vector Machines: A Practical Consequence of Learning Theory”. In: *IEEE Intelligent systems* 13 (1998).

[45] Bernhard Schölkopf et al. “Estimating the support of a high-dimensional distribution”. In: *Neural computation* 13.7 (2001), pp. 1443–1471.

[46] Wei-Cheng Chang, Ching-Pei Lee and Chih-Jen Lin. *A revisit to support vector data description (SVDD)*. Tech. rep. Citeseer, 2013.

[47] David MJ Tax and Robert PW Duin. “Uniform object generation for optimizing one-class classifiers”. In: *The Journal of Machine Learning Research* 2 (2002), pp. 155–173.

[48] Prasanta Chandra Mahalanobis. “On the generalized distance in statistics”. In: *Proceedings of the National Institute of Sciences (Calcutta)* 2 (1936), pp. 49–55.

[49] Arthur Zimek, Erich Schubert and Hans-Peter Kriegel. “A survey on unsupervised outlier detection in high-dimensional numerical data”. In: *Statistical Analysis and Data Mining* 5.5 (2012), pp. 363–387.